Colorimetric Space Study: Application for Line Detection on Airport Areas

Claire Meymandi-Nejad, Esteban Perrotin, Ariane Herbulot, Michel Devy

Colorimetric space study: Application for line detection on airport areas

Claire Meymandi-Nejad[1,2][a], Esteban Perrotin[1,3], Ariane Herbulot[1,4][b] and Michel Devy[1]
[1]*CNRS, LAAS, Toulouse, France*
[2]*INSA de Toulouse, Toulouse, France*
[3]*AIRBUS OPERATIONS S.A.S, Toulouse, France*
[4]*Univ. de Toulouse, UPS, LAAS, F-31400 Toulouse, France*
{*cmeymand, herbulot, devy*}*@laas.fr, esteban.perrotin@airbus.com*

Keywords: color similarity, features extraction, line detection, embedded vision on aircraft

Abstract: We propose an adaptive color reference refinement process for color detection in an aeronautical application: the detection of taxiway markings based on images acquired from an aircraft. Road markings detection is a key functionality for autonomous driving, and is actively studied in the literature. However, few studies have been conducted on aeronautics. Road markings are often detected by using color priors, sensitive to perturbations. Color-based algorithms are still favored in this context as the markings color provides important information. Our proposed method aims at reducing the impact of weather conditions, shadowing and illumination variations on color-based markings detection algorithms. Our approach adapts a given color reference in order to define a new flexible yet robust color reference while maximizing its difference to other colors in the image. It is achieved through a statistical analysis of color similarity over a set of images, computed on several color spaces and distance functions, in order to select the most relevant ones. We validate our approach by analyzing the quantitative improvement induced by this method using two color-based markings detection algorithms, based on the Hough Transform and the Particle Filter.

1 INTRODUCTION

Line detection provides one of the main information required for ADAS (Advanced driver-assistance systems) or for autonomous driving. As such, it is widely present in the automotive field literature (Narote et al., 2018). A good number of studies use a color and/or contrast prior for line detection, where the color space used for this application varies, such as L*a*b* (or CIELAB) in (Kazemi and Baleghi, 2017), HSI in (Sun et al., 2006) or HSV in (Lipski et al., 2008) and (Mammeri et al., 2016). In the automotive field, markings are most of the time white, but their color could vary following the type of road or country. However, most of lane detection applications prefer to convert color images to gray-scale images.

In the context of this study, we focus on aeronautics. We are working on images provided by cameras mounted both in the cockpit and on the tail fin of an aircraft; these images are obtained either from a simulator or from a real aircraft while taxiing. We aim to detect and track markings from each image in order to feed scene understanding methods, such as position and ego-motion estimation, required for autonomous driving. In both domains, there are lines of different colors with different meanings. Converting the image to a gray-scale representation could be misleading and cause confusion, for instance between white and yellow lines. This study concerns the aircraft navigation on taxiways; in this case the color of the markings to be detected is 'yellow'. In aeronautics, the reference color for the 'yellow' markings is defined by the ICAO (International Civil Aviation Organization) requirements (ICAO, 2018) in the xyz color space by color ranges, only valid for a certain illumination level. The yellow color is more difficult to detect than the white and can be easily confused with green, red or light brown that can be found in the airport areas. We need to be able to describe accurately the color differences and similarities of the pixels in our image in order to best detect the markings.

Several studies have been conducted on color similarity and invariance, with multiple color spaces definitions as listed in (Cheng et al., 2001), (Koschan and Abidi, 2008) or (Madenda, 2005) where the author

[a] https://orcid.org/0000-0002-2664-7684
[b] https://orcid.org/0000-0002-8377-6474

presents color similarities between different shades of yellow, based on several distance methods.For line detection in automotive applications, the most widely used color spaces are HSV, HSI and CIELAB, but in this context, we encounter difficulties with the illumination and saturation of the markings color. With the increase of computing resources and image databases, these issues are increasingly addressed in the literature with the development of efficient neural networks such as (Karargyris, 2015) or (Chen et al., 2018) and (Neven et al., 2018), where the first one intends to learn a transform towards a color space that will increase the accuracy of the detection and the two others are focusing on road markings detection. The article (Gowda and Yuan, 2019) concludes that several color spaces, such as RGB, CIELAB or HSV, might increase the classification result on specific classes and that combining some of them could lead to a higher accuracy. One of the objectives of this study is to defined which color space most represents the markings. However, a previous study of the method proposed in (Karargyris, 2015) has not offered satisfactory results on some of our detection works. Also, solid model-based non-linear transforms have been designed in the literature to create complex color spaces models and we do not think that a CNN-based approach will produce an outstanding transform for our problem. A major limitation to the use of neural networks in our application is the lack of a consequent labeled database. Several databases are available in the automotive field but qualitative databases do not exist in aeronautics. This is why we are not currently basing our research on solutions that use CNNs.

An additional difficulty when working with color detection for automotive fields or aeronautical applications comes from the outdoor conditions. The markings colors on the images are affected by shadowing, lightness variation, glare and other impacts of the weather conditions, so that it is mandatory to integrate, in a line detection algorithm, a flexible definition of the reference color for markings. Those perturbations change greatly the color of the markings that diverges from the ICAO requirements and impacts negatively the markings detection.

In this article, in order to improve the detection of the yellow markings in any weather condition, we propose a data-driven method to adapt a given color reference to segregate it in a given context, based on a statistical analysis of the similarity of colors with respect to the reference (here, the ICAO color definition), using several color spaces and color distance functions that we call pairs $(ColorSpace, DistanceMethod)$. We validate this method using two color-based markings detection algorithms, by measuring the quantitative improvement of using the chosen pair. We show that our method increases the robustness of the color segregation to variations in illumination, resulting in a better segmentation on the markings and the tarmac or grass areas, thus a better detection. We chose to focus on the yellow color markings, but this study can be generalized by changing the color reference (for instance the red, white or blue marking colors defined by the ICAO requirements) and recalculating the color distances for each pair. This method can also be used in applications beyond aeronautics context.

In Section 2, we propose a method to refine a color reference by minimizing the distance between this reference and the actual pixels in an image. In Section 3, we analyze several color distance functions in several color spaces, in order to select the most relevant pairs to discriminate a chosen color (here, the ICAO yellow) from others. Section 4 proposes to use the results of this analysis to tune the parameters of the adaptive refinement algorithm. This algorithm is evaluated in Section 5. Finally, we compare two line detection algorithms with and without the automatic reference refinement in Section 6 before concluding about the applicability of the proposed method.

2 COLOR DISTANCE COMPUTATION USING ADAPTIVE REFERENCE

This section presents an algorithm to adapt a color reference to a set of images in order to improve the color segmentation. Since a lot of model-based line detection algorithms are using either binary maps or distance maps, which computation is mostly based on a color processing, the choice of the color reference has a great impact on the final result.

We start from the ICAO color definition that defines the color of the airport markings as a subset of the xyz color space. It is then possible to select a threshold to extract most of the lines from the image. However, images used for this comparison are defined in the sRGB space, while the reference is defined on the full xyz space with specific illumination. Due to evironment perturbations or sensors post-treatments, the color of the markings is sure to vary from this reference color. Hence, we need to apply an empirical modification of this definition, to make it flexible yet as close as possible to the ICAO requirements.

We note $C^* = \{0.45, 0.45, 0.08\}_{xyz}$ the ideal color of the line. We denote $\hat{C}$ the estimator of C^* on the actual image. $\hat{C}$ is computed using a p-Nearest Neigh-

bors algorithm, presented in Algorithm 1. This algorithm requires three parameters: C^*, p the size of the considered neighborhood, and $tolerance$ which define the end criterion. A fourth parameter, $thresh$, is needed to compute the binary map.

Algorithm 1 Color distance computation using adaptive reference.

Require: $p, image, C^*, tolerance, thresh$
  $i = 0$
  $diff = inf$
  $\hat{C}_0 = Convert2ColorSpace(C^*)$
  $image = Convert2ColorSpace(image)$
  while $diff > tolerance$ **do**
    $i = i + 1$
    $dist = Distance(image, \hat{C}_{i-1}))$
    $\vec{x} = GetImageIndexes(sort(dist))$
    $\hat{C}_i = \frac{1}{p} \sum_{k=1}^{p} (image(\vec{x}_k))$
    $diff = Distance(\hat{C}_i, \hat{C}_{i-1})$
  end while
  $dist = Distance(image, \hat{C}_i))$
  $bin = BinarizeDistanceMap(dist, thresh)$
  return $\hat{C}_i, dist, bin$

Before using this algorithm, a Gaussian blur can be performed on the image to remove possible outliers with emphasis on a spatial constraint on the different pixels. It is also used for noise reduction. The proposed algorithm is composed of several steps. Firstly, the RGB color space is not the most efficient color space for color comparison and is not overly used in the literature where HSV and CIELAB color spaces are favored. That is why we perform a conversion to another color space before using the distance function, for example an Euclidean distance. As a result, we obtain a gray-scale image representing the distance map $dist$. In order to refine the reference color, we need to select the pixels that provide the smallest distance value to the reference color. For this purpose, we create a vector of the distances contained in the distance map and select a small number of those pixels defined by p. The new reference color is then updated by the average color of the selected pixels. Those functions are repeated until the color difference between two colors is lesser than the $tolerance$. Finally after this algorithm, the binary map is obtained by thresholding the distance map.

As we work on images that can suffer from the weather conditions or shadowing, we need to find a flexible algorithm that performs well on any image. Hence selecting parameters suitable for any situation. In the following section, we first work on the pairs $(ColorSpace, DistanceMethod)$ to find those that will maximize the discrimination between the reference color and the yellow hues on one part and any other color in the image on the other part in order to select the best distance function to compute the distance map. The selection of the parameters is presented in Section 4 and is dependent on the Section 3 results.

3 STUDY OF COLOR SPACES AND DISTANCE METHODS

This section proposes a statistical analysis of several color representations to select the most relevant ones. The color spaces and associated distance functions considered are described in Table 1.

3.1 Notations

For the rest of this article, for the sake of readability, we will use a common nomenclature for all color distance functions. In addition to the ones referenced in Table 1, we note '$\Delta E_{C_1C_2C_3}$' the Euclidean distances between elements of a given color space, and 'ΔE_{C_i}' or '$\Delta E_{C_iC_j}$' the Euclidean distance computed on a subset of the channels. For instance, we write ΔE_{AB} the Euclidean distance on the A and B channels of the CIELAB color space, or ΔE_H for the Hue channel of the HSV color space. We also note 'ΔC_{LCH}' the weighted Euclidean distance for the LCH color space given by Equation 1, where ΔL and ΔC are the difference between, respectively for the L and C channels, the reference and pixel colors (subscripted $_{ref}$ and $_{pix}$), and δH is a combination of the information given by the C and H channels of the colors.

$$\Delta C_{LCH} = \sqrt{(\Delta L)^2 + (\Delta C)^2 + (\delta H)^2} \qquad (1)$$

$$where \;\; \delta H = \sqrt{C_{ref} * C_{pix}} * 2 * sin(\frac{H_{pix} - H_{ref}}{2}) \quad (2)$$

Table 1: List of color spaces and distances selected for this study, with commonly used notations in parenthesis.

Color Space	Distances
HSV, HSL, XYZ, YCbCr, YIQ	Euclidean distance on all channels
	Euclidean distance on combinations of channels
RGB	Euclidean distance on all channels
	Weighted Euclidean distance on all channels (ΔC)
CIELAB	Euclidean distance on all channels ($\Delta E*_{ab}$)
	Euclidean distance on combinations of channels
	CIE 1994 ($\Delta E*_{94}$)
	CIE 2000 ($\Delta E*_{00}$)
L*C*h	Euclidean distance on all channels
	Euclidean distance on combinations of channels
	CMC l:c 1984 ($\Delta E*_{CMC}$)
	Weighted Euclidean distance on all channels

To select the distance function that best segregate the color of the markings, we need to study the results of several pairs $(ColorSpace, DistanceMethod)$. We call 'color difference' the result of the normalized distance between a color and the reference color provided by the ICAO requirements for a specific pair $(ColorSpace, DistanceMethod)$ as $color\ difference = ||d_{i,E_j}(Ref, PixelColor)||$, where i is the distance method and E_j the color space. Some distance methods being defined only for specific color spaces. The distances are normalized by dividing the color differences by the greatest color difference to the ICAO reference color obtained for each pair.

3.2 Database construction

In order to perform this study on the different distance functions, we decided to create a color database using few real and simulated images provided by an airport simulator. We work with eight images of size 1280pX960p, four images come from cameras mounted on an aircraft and four images come from a simulator. Half of the real and simulated images come from a camera mounted near the cockpit of the aircraft ant the other half come from a camera placed in the fin of the aircraft. Among the eight images, three present degraded weather conditions (fog, dusk, low illumination). All the images are chosen at different areas in the taxiway, with different marking patterns, more or less complex.

We first analyzed the numerous colors present on the selected images. The images can be separated in areas, such as the taxiway (containing most of the gray pixels), the sky (where the majority of the pixels are blue or light colors) and the grass around the taxiway. Most of the colors encountered in the images can be simplified as either 'blue', 'gray', 'green', 'red', 'black' (or dark colors), 'white' (or light colors) or 'yellow' for the markings. We created a database with the unique {R,G,B} triplet of pixels from simulated and real images on several weather conditions, in order to separate the image pixels in different color classes and analyze the performance of all the pairs $(ColorSpace, DistanceMethod)$ in the segregation of the markings color.

As the grass area is composed of a large amount of different colors (green, yellow and brown for example), we defined two subclasses of colors in our classification that we call 'green' and 'grass'. Figure 1 shows an example of one of the images and corresponding masks for the labeling of the pixels for the database. Figure 2 presents the classes that we used for this study and their average proportion in the database and in the images used to construct the database. The colors are ordered by their values on R then G and B. The 'undefined' class represents RGB pixels that have been defined as part of at least 2 classes depending on the images.

3.3 Statistical analysis

We then decided to use multiple criteria to select a subset of candidate pairs that best discriminate the yellow class from the other classes, improving the markings detection:

- The precision for a recall of 100%.
- The precision, recall and F_1 score.
- The dispersion and skewness of the color differences in each class.

Table 2 presents the results of the different pairs based on those criteria for only 18 pairs out of 37. The represented pairs have obtained at least a $+$ on one of the criteria with the exception of ΔE_H that we selected for its results on the box plot (see Figure 3) and also because it is often used for the detection of lines in the literature. From Table 2, we can select three types of methods: those which mostly obtained $+$ on the criteria (such as ΔE_{AB} or $\Delta E*_{CMC}$), those which obtained a mix of $+$ and $=$ (such as ΔE_{IQ} or $\Delta E*_{ab}$) and those which obtained few $+$ and mostly $=$ or $-$ (such as $\Delta E*_{94}$ or ΔE_{HSL}).

For the line *Dispersion and Skewness*, the $+$ value represents pairs which ensure that at least 75% of the color differences of the yellow class can not be confused with another class, the $=$ value represents pairs that could produce a confusion between the yellow class and the gray, red, green or grass classes and the $-$ value lists the pairs which can not be used to segregate the yellow class. In Figure 3, we present a subset of the repartition of the color differences of the cited colors for several pairs. The blue square corresponds to the 25th and 75th percentile and the red line is the median. The lower and upper adjacents (minimum and maximum values that are not considered as outliers) values are given by the black whiskers and the red crosses are the outliers, with their values corresponding to more than 1.5 times the interquartile range. The dotted and dashed lines represent the thresholds reached for the upper adjacent and the 75th percentile of the yellow class.

Figure 3 presents an example of box plot for three pairs: ΔE_{xyz}, ΔE_{CbCr} and ΔE_H that represent 3 sort of results obtained for the 37 pairs. We can see that ΔE_{xyz} can not be used to discriminate the yellow from the other colors even though it is the color space where the reference color for markings is defined, emphasizing our need to find a method to discriminate the reference and yellow colors from other colors in the

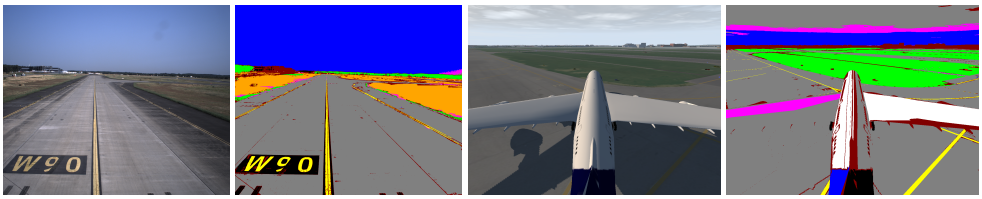

Figure 1: Example of building the database from real and simulated images. Each color mask correspond to one class, with brown for unlabeled pixels, magenta for pixels labeled in several classes and orange for the grass class.

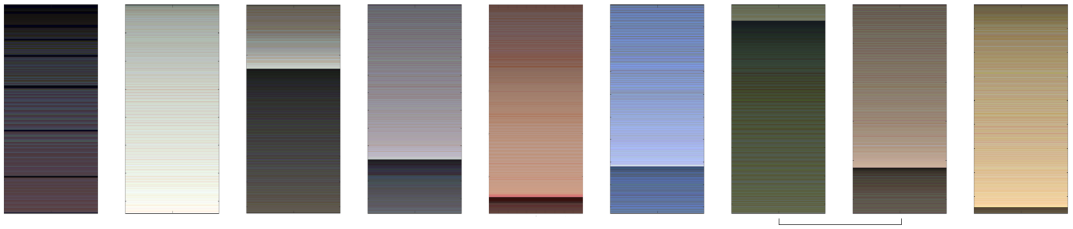

Figure 2: Classes Dark, Light, Undefined, Gray, Red, Blue, Green, Grass and Yellow of the database. Below are the percentages of the representation of the classes (database - image).

Table 2: Comparative table of the performances of several color spaces and distance functions.

	$\Delta E*_{ab}$	ΔE_{AB}	ΔE_{B}	$\Delta E*_{94}$	$\Delta E*_{00}$	ΔE_{LCH}	ΔC_{LCH}	ΔE_{CH}	$\Delta E*_{CMC}$
Precision for $Rec_{100\%}$	=	+	+	+	-	-	+	-	+
Precision for $Rec_{95\%}$	=	+	+	-	-	=	=	+	+
Recall for $Prec_{95\%}$	+	+	+	-	+	+	+	+	+
F_1 Score	+	+	+	=	+	+	+	+	+
Dispersion & Skewness	+	+	+	=	+	=	=	=	+

	ΔE_{HSV}	ΔE_{HSL}	ΔE_{H}(HSL/HSV)	ΔE_{YCbCr}	ΔE_{CbCr}	ΔE_{Cb}	ΔE_{YIQ}	ΔE_{IQ}	ΔE_{I}
Precision for $Rec_{100\%}$	-	-	-	-	+	+	-	+	-
Precision for $Rec_{95\%}$	-	-	=	-	+	+	-	=	=
Recall for $Prec_{95\%}$	=	=	-	=	+	+	=	=	-
F_1 Score	+	+	=	+	+	+	+	+	+
Dispersion & Skewness	-	-	=	-	=	+	-	=	-

image. Some pairs seem to allow the segregation of the yellow color from others, such as ΔE_{CbCr} as most of the classes obtain color differences greater than the 75th percentile of the yellow class. We note that the range of the color difference results is narrower for those methods. However, the yellow class is closely followed by the color differences results from the red and grass classes. For the line detection, it could be a problem as red markings have a completely different meaning than yellow ones and we should avoid the confusion. ΔE_H (on the HSV or HSL color spaces) has a small range of color difference results for the yellow, red, grass and blue classes and can be used to segregate the yellow color. However it also produces a great number of outliers for each class. Those results are consistent with the large shade of hues of each class as can be seen in Figure 2.

Based on the results from Table 2 and Figure 3, we selected a subset of these pairs that we will validate on images that have not been used to create the database:

- $\Delta E*_{ab}$, ΔE_{AB}, ΔE_B and $\Delta E*_{00}$
- ΔE_{LCH}, ΔE_{CH}, $\Delta E*_{CMC}$ and ΔC_{LCH}
- ΔE_{CbCr}, ΔE_{Cb}, ΔE_{IQ}, ΔE_H (HSV/HSL)

4 TUNING OF THE ADAPTIVE ALGORITHM PARAMETERS

Algorithm 1 needs three parameters: p, $tolerance$ and $thresh$. We propose to use the results of the color analysis in Section 3 to fix these parameters.

Figure 2 shows that the colors of the markings represent an average of 1,39% of the pixels in an image, we decided to fix p as 0.1% of the average ratio of the markings colors. This percentage enables us to select

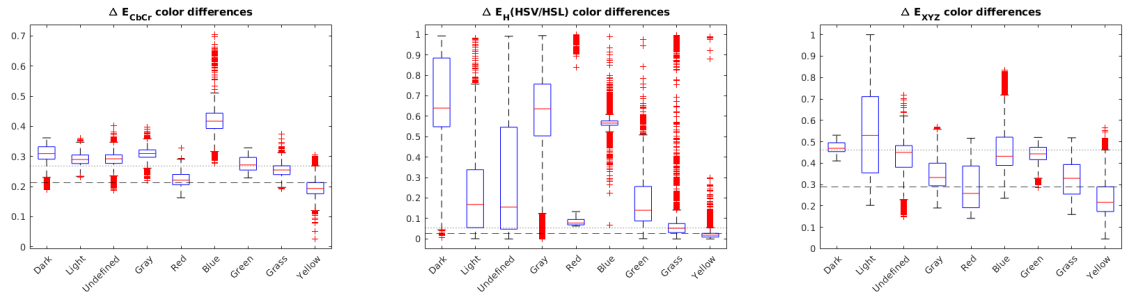

Figure 3: Box plot graphs representing the distribution of the color differences by class for several color spaces and distance functions.

enough pixels to compute a new reference color while minimizing the probability of selecting outliers from other classes that could degrade the reference color.

The purpose of the parameter *thresh* is to create a binary map for the line detection algorithms. To choose how to fix its value, we used the study of the precision, recall and F_1 score of the pairs $(ColorSpace, DistanceMethod)$. A first idea was to use the threshold for which we obtain the best F_1 score in the database analysis. While this threshold maximizes the compromise between precision and recall, it can add outliers to the selection. In this specific context, we decided to use the threshold which corresponds to the loss of the maximum precision, prioritizing the precision over the recall, to minimize the number of selected outliers. Unfortunately, this also leads to a potential increase of the false negatives in the pixels that represent a marking in the image.

The binary map obtained by the thresholding of the distance map is used to analyze the possible number of pixels representing the markings in the image. If the number of detected pixels in the binary map is smaller than p, the algorithm will encounter difficulties to converge to a meaningful reference color. The refinement of the reference color is performed while the color difference is lesser than $tolerance$.

5 EVALUATION OF THE ADAPTIVE ALGORITHM

Thanks to the database study, we selected several pairs as candidates for the distance function in Algorithm 1. We decided to compute the distance and binary maps using each candidate pair $(ColorSpace, DistanceMethod)$ on images not used in the database, both simulated and real, with different weather conditions. The comparison is computed on eight images, selected with the same ratio as the images used for the creation of the database. The binary map is computed by using the parameter *thresh* selected in Section 4.

Figure 4 presents binary and distance maps results for different pairs on a fin camera image and a comparison with the ground truth (last image of the second row). The results of $\Delta E*_{CMC}$, $\Delta E*_{00}$, ΔE_{LCH}, $\Delta E*_{CH}$ and $\Delta E*_{H}$ (HSV/HSL) stand out compared to others. Mostly, any distance method applied to the L*C*h color space gives tangible binary maps.

Table 3 provides results on the precision, recall, F_1 score and accuracy of the binary maps compared to the ground truth, with a reflexion on computation time. The results represent a mean value of the results of the validation images. Several groups of methods appear in Table 3. $\Delta E*_{CMC}$ and ΔE_{LCH} show good results on the different criteria. $\Delta E*_{00}$, ΔC_{LCH}, ΔE_{CH} and ΔE_{H} obtain average results where the other methods are not satisfactory. However the computational time can be an important factor in applications.

As expected, methods with small computational time have worst results than methods with high or average computational time. $\Delta E*_{CMC}$ is the better choice if the computation time is not an important factor but for real time applications ΔE_{LCH} is a good substitute. ΔE_{H} could be selected for high speed computation. We could update the reference color only every second to reduce the impact of the computation time on the selection of the distance function.

When analyzing the color difference to the reference for each class defined in this application, we estimated the precision of the pairs to discriminate the 'Yellow' class. However, we have a representativeness bias in the database because the proportion of each class in the database is different from their proportion in the images, as the triplets' colors are unique in the database. It means that a color of a pixel defined as 'outlier' in the 'gray' class can be labeled as 'Yellow' without a great impact on the pair results.

It could represent a big part of the taxiway in

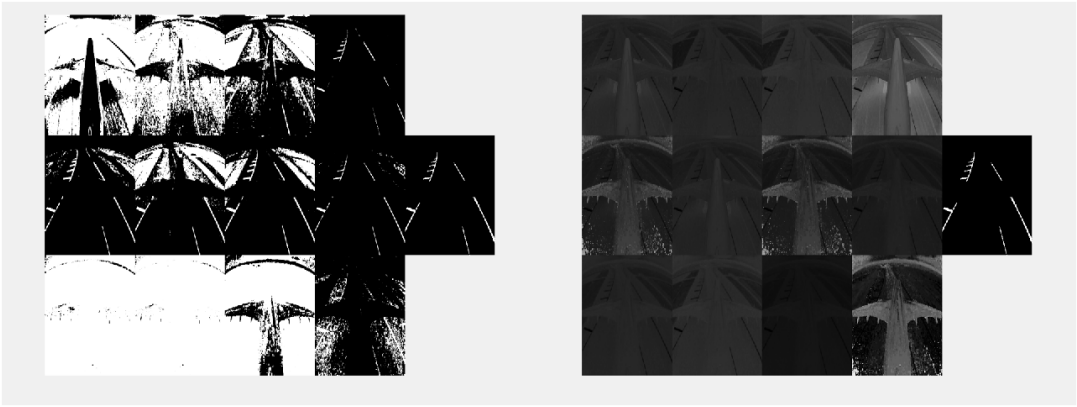

Figure 4: Example of Binary (left) and Distance (right) maps for fin camera images. First line: $\Delta E*_{ab}$, ΔE_{AB}, ΔE_B, $\Delta E*_{00}$. Second line: ΔE_{LCH}, ΔC_{LCH}, ΔE_{CH}, $\Delta E*_{CMC}$, ground truth. Third line: ΔE_{CbCr}, ΔE_{Cb}, ΔE_{IQ}, ΔE_H (HSV/HSL).

Table 3: Comparative table of several color spaces and distance functions on test images (not used in the database).

	$\Delta E*_{ab}$	ΔE_{AB}	ΔE_B	$\Delta E*_{00}$	ΔE_{LCH}	ΔC_{LCH}	ΔE_{CH}	$\Delta E*_{CMC}$	ΔE_{CbCr}	ΔE_{Cb}	ΔE_{IQ}	ΔE_H
Precision	-	-	-	=	=	-	-	+	-	-	-	+
Recall	=	+	+	-	=	=	=	=	+	+	+	-
F_1 score	-	-	-	+	+	=	=	+	-	-	-	-
Accuracy	=	-	-	+	+	=	+	+	-	-	-	+
Computation time	=	=	=	=	=	=	=	-	+	+	+	+

Table 4: Results of line detection algorithms with and without the adaptive refinement of the reference color.

	Recall		Mean Dist		Max Detection		
	HT	PF	HT	PF	HT	PF	GT
cockpit	0.9	0.92	**0.14**	5.22	394	397	607
cockpit adapt. ref.	0.94	**0.96**	3.07	0.71	536	**565**	607
fin	0.34	0.61	11.73	59.02	326	357.7	810.56
fin adapt. ref.	0.58	**0.86**	6.95	**5.94**	**705**	618.5	810.56

the image and modify the performances between the database study and the reference color selection results. This explains why several pairs provided good results during the database study while their resultant distance and binary maps are not satisfying. We could add a weight to our dataset colors to increase the robustness of the classification or add multiples entries of the same (R,G,B) triplets in order to correct this bias partially. We decided to keep this bias in the database and take it into account in the second part of the pairs selection when testing the pairs on global images.

Following the results of Table 3, we decided to select $\Delta E*_{CMC}$. We can note that $\Delta E*_{00}$ gives good results for the binary map. It also gives better results for the distance map than $\Delta E*_{CMC}$ as the contrast between pixels corresponding to the markings and the other pixels is greater. However, this method is less robust on our images.

6 QUANTITATIVE VALIDATION ON LINE DETECTION ALGORITHMS

In order to validate this study, we decided to compare the results for two line detection algorithms: a method based on the Hough Transform as presented in (Hota et al., 2009), called HT in Table 4, and a Particle Filter (PF) implementation (Meymandi-Nejad et al., 2019), on real images only. Both use a color assumption. In order to compare the results of the line detection algorithms with and without using Algorithm 1, we decided to base this analysis on three criteria:

- **Maximum range of detection (in pixels)**: One of the difficulties with our images is that, for fin camera images, the important lines can be found at at least 50 meters from the camera. At this point, the color of the markings is prone to noise and additional saturation which increases its difference from the reference color.
- **Mean of the clusters' pixels' distances to the**

ground truth: it is used as a measure of the algorithm precision. It computes, for each group of pixels, the distance between the potential pixels representing a marking and the ground truth.

- **Recall**

Table 4 shows that all the metrics are improved for both methods by using the adaptive research of the markings reference color. In particular, we note a significant increase in the maximum detection range. The results are more important on the fin camera images because the lines are more blurred and easily confused with the tarmac, particularly when they are far from the camera. We also note an increase of the maximum range detection, directly linked to a better separation between the tarmac and the line.

7 CONCLUSIONS

In this paper, we evaluated several distances between a reference color and pixels of an image, using multiple color spaces, in order to define the pair $(ColorSpace, DistanceMethod)$ that best separate the markings color from the rest of the image. We presented an algorithm to automatically refine this reference color, required for the detection of markings in airport areas. We computed the distance between the reference color and the color of every pixel in the image, providing either a binary image with pixels classified as 'markings' or a distance map; these outputs are exploited by two line detection algorithms, based on the Hough transform or the Particle Filter. We observed a clear improvement of their results when using the adaptive refinement of the reference color.

Such a method can be used, for instance, to detect several markings in the airport areas such as beacons or other colors of lines by modifying the reference color and re-running the database and robustness to noise studies. Assuming the use of neural networks on a prospective study, it could be interesting to compare the results of changing the RGB image to a L*C*h image as an input of the network on the detection results. In this study, we worked with known color spaces without defining an order relation between their channels. Future works could include an algorithm as proposed in (Lambert and Chanussot, 2000), to improve the yellow boundaries detection process while adding an order relation between the channels of the different color spaces. It could also be interesting to use CNNs to deal with more complex classifications such as non-linear separators, taking into account the concerns about the certifications problems.

REFERENCES

Chen, P., Lo, S., Hang, H., Chan, S., and Lin, J. (2018). Efficient road lane marking detection with deep learning. In *2018 IEEE 23rd International Conference on Digital Signal Processing (DSP)*.

Cheng, H., Jiang, X., Sun, Y., and Wang, J. (2001). Color image segmentation: Advances and prospects. *Pattern Recognition*.

Gowda, S. N. and Yuan, C. (2019). Colornet: Investigating the importance of color spaces for image classification. In *Computer Vision – ACCV 2018*.

Hota, R. N., Syed, S., Bandyopadhyay, S., and Krishna, P. R. (2009). A simple and efficient lane detection using clustering and weighted regression. In *COMAD*.

ICAO (2018). *AERODROMES: aerodromes design and operations.*

Karargyris, A. (2015). Color space transformation network. *arXiv*.

Kazemi, M. and Baleghi, Y. (2017). L*a*b* color model based road lane detection in autonomous vehicles. *Intelligent Transportation Systems (ITS)*.

Koschan, A. and Abidi, M. (2008). *Digital color image processing*. John Wiley & Sons.

Lambert, P. and Chanussot, J. (2000). Extending mathematical morphology to color image processing. *Proc. CGIP*.

Lipski, C., Scholz, B., Berger, K., Linz, C., Stich, T., and Magnor, M. (2008). A fast and robust approach to lane marking detection and lane tracking. *IEEE Southwest Symposium on Image Analysis and Interpretation*.

Madenda, S. (2005). A new perceptually uniform color space with associated color similarity measure for content-based image and video retrieval. *Multimedia Information Retrieval Workshop, 28th Annual ACM SIGIR Conference*.

Mammeri, A., Boukerche, A., and Tang, Z. (2016). A real-time lane marking localization, tracking and communication system. *Computer Communications*.

Meymandi-Nejad, C., Kaddaoui, S. E., Devy, M., and Herbulot, A. (2019). Lane detection and scene interpretation by particle filter in airport areas. In *International Conference on Computer Vision Theory and Applications*.

Narote, S. P., Bhujbal, P. N., Narote, A. S., and Dhane, D. M. (2018). A review of recent advances in lane detection and departure warning system. *Pattern Recognition*.

Neven, D., Brabandere, B. D., Georgoulis, S., Proesmans, M., and Gool, L. V. (2018). Towards end-to-end lane detection: an instance segmentation approach. *IEEE Intelligent Vehicles Symposium*.

Sun, T.-Y., Tsai, S.-J., and Chan, V. (2006). Hsi color model based lane-marking detection. *IEEE Intelligent Transportation Systems Conference*.